Chiral Discrimination in Host–Guest Supramolecular Complexes. Understanding Enantioselectivity and Solid Solution Behaviors by Using Spectroscopic Methods and Chemical Sensors

ARTICLE *in* THE JOURNAL OF PHYSICAL CHEMISTRY B · JULY 2007

Impact Factor: 3.3 · DOI: 10.1021/jp071428o · Source: PubMed

6 AUTHORS, INCLUDING:

Arnaud Grandeury
Novartis
17 PUBLICATIONS **93** CITATIONS
SEE PROFILE

Eric Condamine
French National Centre for Scientific Research
46 PUBLICATIONS **461** CITATIONS
SEE PROFILE

L. Hilfert
Otto-von-Guericke-Universität Magdeburg
43 PUBLICATIONS **341** CITATIONS
SEE PROFILE

Gérard Coquerel
Université de Rouen
197 PUBLICATIONS **1,526** CITATIONS
SEE PROFILE

Chiral Discrimination in Host−Guest Supramolecular Complexes. Understanding Enantioselectivity and Solid Solution Behaviors by Using Spectroscopic Methods and Chemical Sensors

Arnaud Grandeury,[†,‡] Eric Condamine,[§] Liane Hilfert,[||] Géraldine Gouhier,[+] Samuel Petit,[*,†] and Gérard Coquerel[†]

Unité de Croissance Cristalline et de Modélisation Moléculaire, Sciences et Méthodes Séparatives, UPRES EA 3233, IRCOF, Université de Rouen, F-76821 Mont Saint-Aignan Cedex, France, Laboratoire de Chimie Organique et Biologique Structurale, UMR CNRS 6014, IRCOF, Université de Rouen, F-76821 Mont Saint-Aignan Cedex, France, Chemisches Institut, Otto-von-Guericke-Universität, Universitätsplatz 2, D-39106 Magdeburg, Germany, and Equipe des Fonctions Azotées et Oxygénées Complexes, UMR CNRS 6014, IRCOF, Université de Rouen, F-76821 Mont Saint-Aignan Cedex, France

Received: February 20, 2007; In Final Form: April 13, 2007

Diastereomeric host−guest associations formed between permethylated-β-cyclodextrin (TMβ-Cd) and the two enantiomers of *p*-bromophenylethanol (*p*BrPE) were characterized in aqueous solution by NMR spectroscopy, revealing similar inclusion geometries and weak binding constants, whatever the guest configuration. These features were confirmed by hydrogenation experiments, and do not allow to account for the ability of TMβ-Cd to resolve racemic *p*BrPE by successive crystallizations [Grandeury, A.; Petit, S.; Gouhier, G.; Agasse, V.; Coquerel, G. *Tetrahedron: Asymmetry* **2003**, *14*, 2143−2152]. The analysis, by means of solid-state NMR, oxidation experiments, and solubility measurements, of the two crystalline phases containing known proportions of guest enantiomers revealed identical inclusion geometries in a given phase, irrespective of the enantiomeric composition. The corresponding solid solutions were further characterized by the determination of an isothermal section (40 °C) in the relevant ternary phase diagram. It appears from all these data that chiral resolution mechanisms in this system can only be envisaged in terms of nucleation conditions of each crystal form (with its specific inclusion geometry) and enantiomeric recognition at crystal solution interfaces during the growth of each crystal packing.

I. Introduction

Chiral recognition phenomena are of primary importance in most living systems and in chemistry. The underlying mechanisms are not yet fully identified, although general tendencies have emerged, involving for instance shape complementarities in the case of host−guest systems, or optimal contact areas in the frame of the lock and key concept.[1] Progress in investigation techniques, such as multidimensional and solid-state NMR spectroscopies, or single-crystal X-ray diffraction methods have provided insights at a molecular level on stereodifferentiation and related discrimination effects.

Cyclodextrins (Cds hereafter) have often been employed as reference host compounds in supramolecular chemistry, due to their well-defined hydrophobic cavity that can contain (partially or completely) various organic, inorganic and biological molecules, leading to stable inclusion complexes.[2] These macrocyclic molecules are obtained by enzymatic degradation of starch and consist mainly of six (α-Cd), seven (β-Cd) or eight (γ-Cd) alpha-(1 → 4) linked D-glucopyranose units.[3] The stabilization of host−guest inclusion complexes can involve several types of intermolecular interactions such as hydrogen bonds, van der Waals forces, strain energy of the macrocyclic ring, and hydrophobic or dipolar interactions.[4]

Native cyclodextrins can be chemically modified in order to enhance some of their properties.[5] In particular, the partial or complete methylation of hydroxyl functions has been identified as an important factor to increase their chiral recognition capacities, mainly in chromatographic sciences. The basic principle of enantiorecognition is supposed to involve the formation of diastereomeric complexes exhibiting different physical properties.

In contrast with the abundant literature dealing with the efficiency of cyclodextrins for enantioseparation in analytical chemistry, only few papers have reported their use for chiral resolutions at a preparative scale through crystallization procedures. Most of the enantioenrichments reported with native Cds are weak,[6−8] and this poor efficiency has been attributed to their high molecular rigidity since the intramolecular hydrogen bond network is assumed to reduce the possibility of host−guest conformational adjustment ("induced-fit").[9]

In order to circumvent this problem, the formation of dimeric host capsules (2:1 Cds:guest) provides an efficient alternative strategy when the guest geometry allows the formation of such multicomponent species.[7] This approach is based on different microscopic binding constants between the different complexes,

* Corresponding author. Tel.: +33.(0)2.35.52.24.28. Fax: +33.(0)2.35.52.29.59. E-mail: samuel.petit@univ-rouen.fr.

† Unité de Croissance Cristalline et de Modélisation Moléculaire, Sciences et Méthodes Séparatives, Université de Rouen.

‡ Present address: Cephalon France, Chemical Process R&D, Rue E. Branly, ZI Mitry Compans, F-77292 Mitry Mory Cedex, France.

§ Laboratoire de Chimie Organique et Biologique Structurale, Université de Rouen.

|| Otto-von-Guericke-Universität.

+ Equipe des Fonctions Azotées et Oxygénées Complexes, Université de Rouen.

10.1021/jp071428o CCC: $37.00
Published on Web 06/05/2007

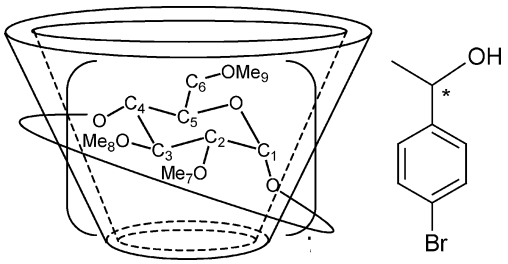

Figure 1. Molecular structure of permethylated β-cyclodextrin (TMβ-Cd, left) and *p*-bromophenylethanol (*p*BrPE, right).

and chiral discrimination is supposed to be induced by the population repartition between the different species in solution (free components, 1:1 and 2:1 complexes). An interesting aspect in this strategy is that the efficiency of the resolution can be predicted by considering the relative ratio between these microscopic constants. However, such an approach does not consider the asymmetry of physical properties between diastereomeric species, as well as the eventual discrimination effects induced by crystallization mechanisms.[10]

Compared to native Cds, a higher ability of permethylated cyclodextrins (TM-Cds) for crystallization-induced stereorecognition has been highlighted.[9] Indeed, the full methylation of hydroxyl groups facilitates the molecular adjustment of the host and reduces the penetration of the guest molecule inside the cavity.[11] In the solid state, a higher amount of selective intermolecular interactions between the guest and its chiral environment may be reached, including favorable contacts with neighboring components in the crystal lattice. However, the chiral discrimination ability of TM-Cds in crystallized materials has been investigated and established only with a limited number of guest molecules.[9,12−14]

With the aim to understand some fundamental aspects of chiral discrimination by means of supramolecular complexation, we have recently studied the crystallization behavior of host−guest complexes formed with TM-Cds.[15−17] Using as model compounds a homologous series of racemic *p*-halogenated derivatives of phenylethanol, we have shown that enantiomeric enrichments obtained by crystallization depend on kinetic parameters, since the optical purity of the obtained solids are in most cases significantly affected by crystallization durations.[15] The existence of partial or complete solid solutions between diastereomeric complexes obviously reduces the efficiency of the enantiomeric separation process, but does not impede chiral discrimination. Indeed, we have demonstrated for two different guest compounds that complete resolutions can be achieved by means of successive crystallizations.[16,17]

An interesting behavior observed in the course of these investigations is that of complexes formed between permethylated β-cyclodextrin (TMβ-Cd) and *p*-bromophenylethanol (*p*BrPE) (Figure 1). In this system involving the solvent (water), the host molecule, and the two guest enantiomers, two different crystalline phases have been detected and characterized by means of various techniques, including single-crystal X-ray diffraction.[16] Each phase exhibits specific supramolecular features and distinct inclusion geometries of guest molecules with the bromine atom located either on the upper side of the tore (orthorhombic form, called phase α hereafter) or engulfed at the bottom of the cavity of the macrocycle (monoclinic form, phase β hereafter) (Figure 2).

Although enantiomeric excesses (e.e.) in single crystals are limited to ca. 60% and 40% for (*S*)- and (*R*)-*p*BrPE respectively, the presence of the counter enantiomer has not been detected during the last refinement steps of crystal structure determinations.[16] It can therefore be expected, owing to the high electronic density of the bromine atom, that a unique inclusion geometry is imposed by each crystal packing (Figure 3). A careful examination of intermolecular interactions between host and guest components in these structures revealed that no additional contacts exist between each guest molecule and neighboring building blocks in the crystal lattice, whatever the considered geometry. Therefore, selectivity during crystallization may derive from the individual recognition of each supramolecular complex and from solubility differences. Molecular modeling calculations for the two inclusion geometries revealed only weak energy differences between the different guest configurations.[16] Consequently, it can be postulated that different types of host−guest associations should pre-exist in solution.

In order to investigate further the role of nucleation and crystal growth in chiral recognition mechanisms, the *p*BrPE/TMβ-Cd system has been characterized in aqueous solution. A complementary study of inclusion geometries in the solid state is also

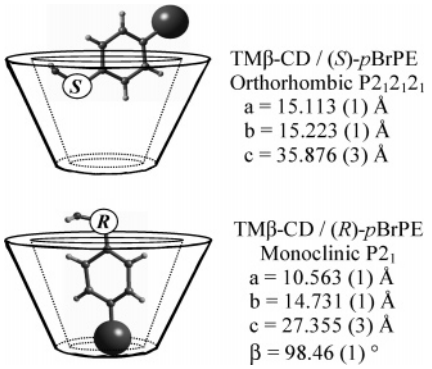

Figure 2. Crystallographic parameters and schematic representation of the inclusion geometry of (*S*)- (upper, phase α) and (*R*)- (lower, phase β) *p*BrPE in the TMβ-Cd cavity, deduced from single-crystal X-ray analysis.[16]

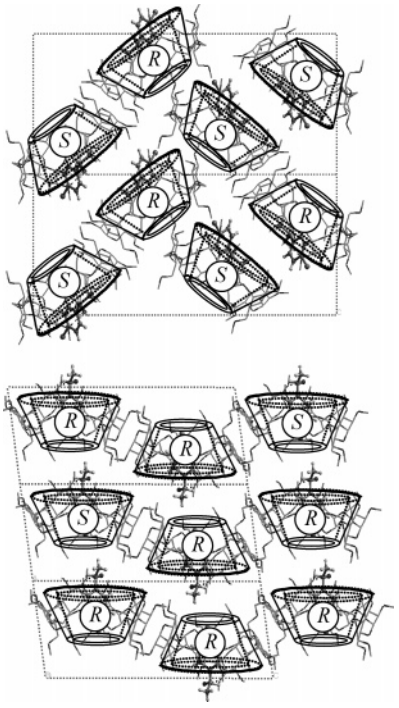

Figure 3. Hypothetical structural features of solid solutions α (upper) and β (lower) consisting of homogeneous inclusion geometries. Packings are deduced from crystal structures with pure enantiomers (α:(*S*); β:(*R*))[16] and guest configurations have been randomly attributed.

reported here, with the aim to identify relationships between species existing in solution and in crystalline samples.

II. Experimental Methods

II.1. Materials. Commercial TMβ-Cd monohydrate of high purity (>97%) was purchased from Cyclolab Inc. (Budapest, Hungary) and used without further purification. Racemic 1-(*p*-bromophenyl)ethanol was obtained by reduction of the corresponding ketone. Pure enantiomers of *p*BrPE were obtained by a partial asymmetric reduction, followed by a kinetic oxidation, and the corresponding alcohols with the required enantiomeric purity (e.e.>99%) were easily isolated.[18] Supramolecular complexes were prepared according to a previously detailed procedure.[15]

II.2. Analytical Methods and Physical Characterization of Solid-State Samples. Enantiomeric compositions of *p*BrPE in complexes were determined from chiral gas chromatography analyses performed on a Packard 5890 instrument equipped with a Supelco Betadex column (140 °C, isothermal run, injector and detector temperature 250 °C, Helium carrier gas, μ_{opt}= 30 cm.s^{-1}). X-ray powder diffraction (XRPD) patterns were recorded on a Siemens D5005 diffractometer (Cu Kα). Solubility values were determined by the gravimetric method (at least two independent measurements).

II.3. NMR Methods. Intermolecular dipolar interactions were investigated on a Bruker Avance DMX 500 NMR spectrometer. ^{1}H and ^{13}C signals assignment was achieved using ^{1}H-^{1}H COSY,[19] ^{1}H-^{13}C HSQC[20], and ^{1}H-^{13}C HMBC[21] experiments. ^{1}H-^{1}H NOESY[22] and T-ROESY[23] (with TOCSY suppression) were used concomitantly to crosscheck for peaks resulting from coherent or mixed magnetization transfer or loss of NOE information in $\omega\tau_c = 1$ domain. ^{1}H spin−lattice relaxation times (T_1) were evaluated using inversion−recovery sequence.[24] Several ^{1}H-^{1}H T-ROESY experiments with different spin-lock mixing times in the range of T_1 were recorded to ensure the validity of the linear approximation for the ROE cross-peaks and to obtain the best signal-to-noise ratio. Spatial proximities of protons were deduced from cross-peak integrations of T-ROESY spectra recorded with a spin-lock mixing time of 500 ms at 20 °C. Samples were prepared using well-characterized crystalline supramolecular complexes, dissolved in D_2O (final concentrations were 10 mM). Several freeze−pump−thaw cycles were used to minimize residual dioxygen in solution.

Titration experiments were performed on a Bruker ARX 400. Two solutions were mixed in different ratios (500 μL/0 μL; 450 μL/50 μL; ...; 0 μL/500 μL). The initial composition of each solution was about exactly 10 mM of 1:1 supramolecular complexes and about exactly 10 mM of TMβ-CD alone in order to keep constant the host concentration. Spectra were referenced to the TMS peak calibrated to 0 ppm, TMS being introduced in a separate coaxial capillary tube and therefore used as an external reference (1 mM in D_2O).

The ^{13}C CP-MAS spectra were recorded on a Bruker Avance 300 NMR spectrometer operating at 75.47 MHz. The spectrometer was equipped with a 4 mm CP/MAS probehead BL4. The proton 90° pulse was set to 3.6 μs, and the decoupling strength during acquisition was 69 kHz. The following conditions were applied: 5 kHz spinning rate, recycle delay of 15 s, contact time 5 ms. The samples were introduced in 4 mm ZrO_2 rotors. Chemical shifts are quoted in parts per million from TMS.

II.4. Hydrogenation of pBrPE in Water. For this reaction, 500 mg (0.31 mmol) of crystalline supramolecular complexes was dissolved in 10 mL of distillated water. Then, 0.6 mL of Ni Raney purchased as an aqueous slurry, and preliminarily washed twice in saturated sodium hydrogenocarbonate, was introduced under stirring. The solution was maintained at 40 °C for 2 h, and then filtrated over celite, washed, and extracted with 3 × 10 mL of diethylether. The organic phases were dried over $MgSO_4$, and concentrated under vacuum. About 36 mg of phenylethanol (0.29 mmol, 95%) were isolated by flash chromatography (cyclohexane/ethyl acetate: 85/15).

TABLE 1: Relative Cross-Peak Intensities from T-ROESY Experiments for Supramolecular Complexes Formed between TMβ-Cd and Each Enantiomer of *p*BrPE at 20 °C[a]

		TMβ-Cd/(*S*)-*p*BrPE	TMβ-Cd/(*R*)-*p*BrPE
strong ROE	H5g/H5h	23	22
	H4g/H5h	13	12
	H5g/H3h	10	*c*
medium ROE	H4g/H3h	6	*c*
	H4g/H8h	6	*c*
	H5g/H8h	4	*c*
	H4g/H8h+H3h	24[b]	21[b]
	H5g/H8h+H3h	21[b]	17[b]

[a] Intensities are reported in an arbitrary unit based on ratios: H4g/H2g = 20 and H4g/H1g = 3; a corrective factor for the methyl groups contribution has been applied. [b] Without corrective factor for comparison with superimposed signals [c] Superimposition of H3h and H8h signals.

II.5. Oxidation of pBrPE at the Solid State Using Microwave (MW) Irradiation. First, 380 mg (0.23 mmol) of supramolecular complexes formed between TMβ-Cd and *p*BrPE in a 1:1 ratio was crushed over 30 min until amorphization (checked by XRPD analysis). Iodobenzendiacetate (740 mg, 2.3 mmol, 10 eq.) was added and crushed with the complexes during a few minutes. The resulting powder was introduced in a tube adapted to the microwave, and the sample was exposed to a focused MW irradiation (SEM DiscoverTM Magnetron frequency 2455 MHz) without considering any temperature restriction 100 W/60 min. The crude product was purified by flash chromatography (cyclohexane/ethylacetate: 85:15). The yields depend on the nature of the initial crystal packing.

III. Results and Discussion

III.1. Investigations in Solution. *III.1.1. Inclusion Geometries.* Structural data of (*R*)- and (*S*)-*p*BrPE/TMβ-Cd diastereomeric complexes in the solvated state were deduced from ^{1}H-^{1}H T-ROESY experiments (rotating-frame NOE with TOCSY suppression) performed in deuteriated water at 20 °C. This technique is known to provide the most reliable information about the relative interproton distances in compounds of intermediate molecular weight[25] and has been successfully applied for a similar purpose in the case of supramolecular complexes formed between TMβ-Cd and binaphthyl derivatives.[12] Since previous structural data were obtained using single crystals grown at 40 °C (due to the retrograde solubility of these compounds),[26] it has been checked that similar crystallization behaviors are observed at 20 and 40 °C, allowing us to confirm that identical phenomena take place in terms of spontaneous enantiomeric enrichment in close-to-equilibrium conditions and successive formation of distinct crystalline phases.

For the two diastereomeric complexes, the T-ROESY spectra showed cross-peaks between the aromatic protons of *p*BrPE and macrocycle protons located inside the cavity, whereas no significant cross-peaks were observed with outer protons, confirming the formation of inclusion complexes in solution (Table 1, see Figure 4 for proton numbering). However, due to the superimposition of some signals in the sample containing the (*R*) enantiomer of *p*BrPE, the individual correlation of H3h

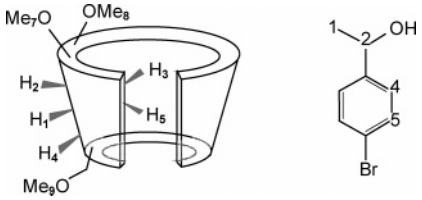

Figure 4. Identification of host (h, left) and guest (g, right) protons for analysis of NMR experiments in solution (see Table 1).

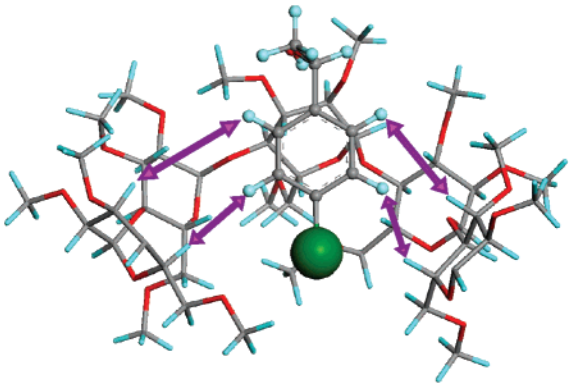

Figure 5. Schematic representation of supramolecular complexes in deuteriated water formed between TMβ-Cd and *p*BrPE, whatever the guest chirality, as deduced from ROESY experiments at 20 °C (the arrows indicate the strongest correlation; the Cd cavity is clipped at the front to show clearly the inclusion).

and H8h cannot be easily deduced. Cross-peak volumes were integrated and normalized against the same reference for the two diastereomeric complexes and a corrective factor for methoxy groups contribution has been applied, allowing the comparison of the collected data. Surprisingly, this analysis revealed almost similar interactions between host and guest components, whatever the guest configuration.

The strong intermolecular ROE signals between protons located inside the cavity (H3h and H5h) and those of the aromatic ring (H4g and H5g) are consistent with an inclusion geometry in which the bromine atom and the aromatic ring are engulfed in the Cd cavity. The main molecular axis of *p*BrPE is then almost parallel to the pseudo 7-fold axis of TMβ-Cd and the corresponding correlations are represented in Figure 5.

Although this pattern represents the supramolecular conformation in which the hydrophobic moiety of the guest minimizes its contact surface with the polar solvent, the absence of differentiation between the two guest enantiomers does not reflect the behavior observed in the solid state, where different inclusion geometries have been well-characterized. Since NMR data reveal only the predominant position of the guest at the average time scale of the NMR measurements, one should not exclude the existence of other host−guest geometries in solution, in particular when the concentration is increased. Even so, such behavior is unexpected since it is usually assumed that the inclusion geometry of host−guest complexes depicted in the crystal lattice is similar to that existing in solution. A similar discrepancy has been reported in the case of supramolecular complexes formed between α-Cd and achiral 4-fluorophenol.[27] In this system, the distinct geometries depicted in solution and in the solid state are assumed to be the most stable for a given environment in each phase, and have been explained from molecular modeling simulations.[28] In the present case, both geometries can be obtained spontaneously in the solid state, indicating that the influence of the molecular environment should involve additional discrimination mechanisms related to

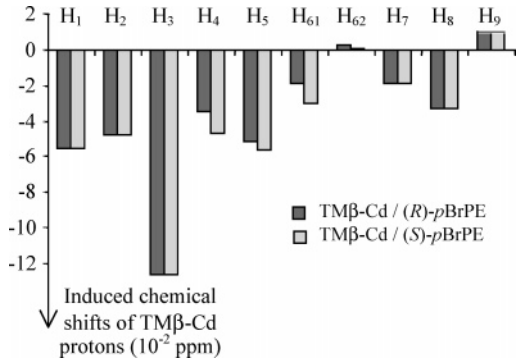

Figure 6. Complexation induced chemical shifts for TMβ-Cd and each enantiomer of *p*BrPE in 1:1 ratio at 10 mM in D_2O (for peak identification, see Figure 4).

the chiral configuration of the guest itself, and able to influence significantly the nucleation step.

The above results, supporting the existence of a dominant self-association geometry in solution irrespective of the guest chirality, have been confirmed by circular dichroism (CD) (see Supporting Information), since the butterfly shape of the CD spectra indicates similar molecular environments in solution, whatever the diastereomeric composition.

III.1.2. Binding Constants. In order to quantify a possible discrimination in solution, the binding association constants of the two diastereomeric complexes have been determined by NMR titrations in deuteriated water at 25 °C through a monitoring of the chemical shift of the H5g proton (equations and fitting procedures are included in the Supporting Information).[29]

The measured binding constants are 162 (±32) L.mol^{-1} for (*S*)-*p*BrPE/TMβ-Cd and 153 (±30) L.mol^{-1} for (*R*)-*p*BrPE/TMβ-Cd. Despite relatively large experimental uncertainties caused by the conjugated effects of weak binding constants and limited solubilities, some general tendencies can be deduced. It should be first highlighted that binding constants are unexpectedly low, referred to the hydrophobic character of *p*BrPE and to its complete solubilization in the presence of one molar equivalent of TMβ-Cd in water.[15] Indeed, the guest compound is almost non miscible with water, so the presence of a large proportion of dissociated complexes in solution should be associated to the formation of an emulsion at the working concentration. This apparent contradiction can only be solved by assuming the existence of solvated molecular clusters in which guest molecules are located in interstitial cavities existing between neighboring host molecules, so as to avoid direct contacts with water. In this configuration, guests are therefore not included in the cavity of macrocycles but rather engulfed in nanoscopic areas formed by at least 3−4 macrocyclic hosts. Such a supramolecular organization has actually been observed at the solid state in the crystal structure of a complex formed between TMβ-Cd and *p*-iodophenylethanol (data to be published).

In terms of stereodifferentiation, the weak difference detected between the two pure complexes indicate a poor recognition phenomenon,[30] and the experimental uncertainties do not allow to conclude on the existence of any significant chiral discrimination in the solvated state. This is confirmed by the comparison of specific chemical shifts caused by diastereomeric host−guest interactions in the 1D ^{1}H spectrum (Figure 6).

Attempts to obtain more significant data were performed using isothermal titration calorimetry, since this technique is known to be reliable in the case of weak binding constants.[31]

SCHEME 1: Hydrogenation of *p*BrPE Using Ni Raney, Allowing Evaluation of the Dissociation State of Solvated "Host−Guest" Supramolecular Complexes

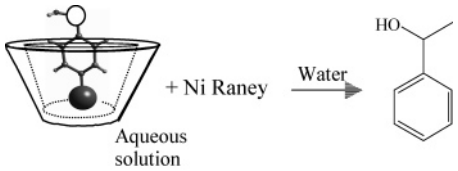

Substrate	Yield
TMβ-Cd / (*S*)-*p*BrPE	95%
TMβ-Cd / (*R*)-*p*BrPE	95%
(±) *p*BrPE (alone)	95%

However, these experiments were unsuccessful due to the low solubility of the aromatic guest in water and to large heats of dilution of the host molecule.

III.1.3. Geometry of Dissociated Complexes. The weak binding constants depicted above imply that a large proportion of free solvated molecules (host and guest) are in dynamic equilibrium with the corresponding complexes. Indeed, considering the solubility values at 40 °C (in the range 10−20 mM, depending on complex composition), a binding constant of 150 L.mol^{-1} reflects a dissociation rate of host−guest entities close to 45%.

Despite this low proportion of inclusion complexation in solution, significant host−guest interactions should however exist in solution between components since dissolution of the supramolecular complexes in water does not induce the formation of an emulsion (*p*BrPE alone is scarcely soluble in water). In order to investigate further the dissociated state in aqueous solution, the accessibility of the bromine atom has been evaluated by hydrogenation using Ni Raney (Scheme 1).[32] The reaction usually involves a Ni alloy in an aqueous solution saturated with sodium hydrogenocarbonate. In order to avoid any modification of binding constants due to ionic strength changes,[33] the reaction conditions in aqueous solution have been first optimized in the absence of host molecules, and ground Ni Raney appeared to be more efficient than the different alloys tested. After a pre-activation step in basic medium and washing, phenylethanol can be isolated with 95% yield after 2 h. A similar procedure applied to the supramolecular complexes formed between TMβ-Cd and pure (*S*)- and (*R*)-*p*BrPE allows hydrogenation with similar yields but requires longer reaction durations (4 h). Owing to the inclusion geometry of the complexed state deduced from NMR analysis in solution, the C_{ar}−Br bond should be protected. The high yields obtained reveal that associated and dissociated species are probably involved in a fast and dynamic equilibrium in solution, making the halogen atom accessible.

Hence, although a predominant host−guest geometry in aqueous solution has been characterized as a true inclusion complex with the aromatic moiety of the guest engulfed in the cyclodextrin cavity, the weak binding constants and the large mobility of components suggest that the crystal growth of each diastereomeric compound should involve a reassociation phenomenon occurring at crystal−solution interfaces, with the required inclusion geometry.

Furthermore, attempts to establish the existence of a chiral recognition revealed a poor ability of the host to distinguish the enantiomers of *p*BrPE in the solvated state. This does not allow to account for the significant selectivity observed upon crystallization. This behavior differs from that described in the literature, where the selectivity observed in the solid state is often related to a chiral discrimination pre-existing in solution.[7,12,13]

III.2. Investigations at the Solid State. *III.2.1 Solid-State NMR Analysis.* Previous crystal growth and structural investigations have established that, despite the existence of genuine diastereomeric compounds, crystal packings are able to incorporate various proportions of the other enantiomer.[15] However, X-ray diffraction techniques could not provide information about the inclusion geometry of complexes containing "counter enantiomer" guest molecules. Solid-state ^{13}C cross-polarization magic-angle spinning (^{13}C CP-MAS) NMR was therefore used as a complementary technique for the study of crystalline samples of known e.e. and crystal packing (Figure 7).[34]

For comparative purpose, TMβ-Cd monohydrate was also analyzed by ^{13}C CP-MAS NMR. Its spectrum revealed a more complicated profile than that obtained in solution, probably due to the molecular asymmetry of the macrocycle (Figure 7a). In aqueous medium, each glucosidic unit contributes to the same chemical shift in a statistically symmetric structure (only 9 peaks),[35] whereas the existence in the solid state of multiple resonances for each type of carbon atom is a consequence of different torsion and tilt angles.[10,36] Furthermore, signal attribution is difficult to establish because of a widening of chemical shifts. The most important dispersion is observed for the C_1 chemically equivalent carbons (see Figure 1 for atom labeling) that exhibit differences up to 15 ppm (85−100 ppm) probably caused by the unusual conformation of one glucosidic unit with a $^1C_4$ conformation in this monohydrated structure.[37]

Spectra of phase α (orthorhombic crystal form, see Figures 2 and 3) exhibit distinct features compared to the host alone, but does not seem to be sensitive to the optical purity. Indeed, despite a satisfactory resolution and the absence of split, no broadening or additional peaks are detected in the spectrum obtained for the sample containing the two guest enantiomers (Figure 7b,c). The good resolution of signals suggests weak host−guest interactions in the solid state.[38,39] Only the aromatic carbon signals of the guest (135−127 ppm) are not well-resolved and weak. This can reflect an anisotropy of the molecular environment (potentially attributed to a local agitation along the molecular axis of the aromatic ring) or to a longer relaxation time of the nuclei.

For phase β (monoclinic crystal form, see Figures 2 and 3), the spectra differ from that of phase α, although similar conformational features of the macrocycle have been reported from crystal structure descriptions (Figure 7d,e).[16] Therefore, chemical shifts of host molecules are not only affected by their conformations, but also by the inclusion geometry of the guest, and/or the crystal packing. As in the case of phase α, no differentiation related to guest configuration is observed. The most important signature of the studied phases (α and β) is the signal attributed to the methyl group of guest molecules (C1g), with specific chemical shifts (δ = 28.55/29.95 ppm for phases α and β respectively) and different shapes. In order to evaluate the sensitivity of these analyses, physical mixtures of different optically pure crystalline phases (initial ratio 40/60 (α/β)) have been analyzed and correspond to the superimposition of each individual spectrum (Figure 7f).

Consistent with structural data obtained by single-crystal X-ray diffraction, solid-state NMR spectroscopy indicates specific features for the two crystal forms, and supports the hypothesis of a single inclusion geometry. However, it does not allow to distinguish the handedness of the guest molecule

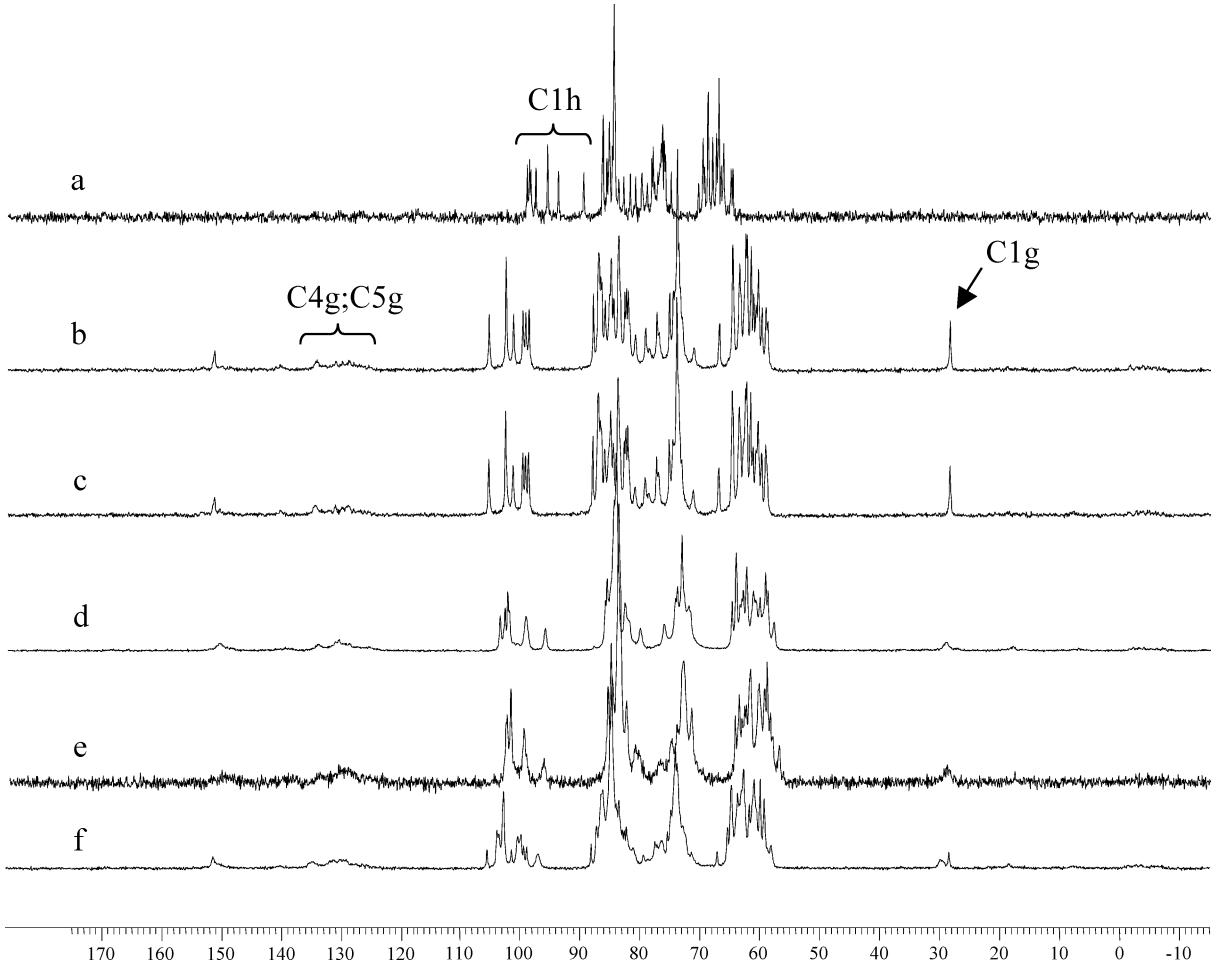

Figure 7. ^{13}C CP-MAS NMR spectra of crystalline supramolecular species: (a) TMβ-Cd, monohydrate; (b) TMβ-Cd/(*S*)-*p*BrPE (phase α); (c) TMβ-Cd/(*S*)-*p*BrPE e.e. = 45% (phase α); (d) TMβ-Cd/(*R*)-*p*BrPE (phase β); (e) TMβ-Cd/(*S*)-*p*BrPE e.e = 25% (phase β); (f) physical mixture of enantiopure phases α and β (0.4:0.6).

through the presence of specific signals for samples containing the two guest enantiomers.

III.2.2. Oxidation as a Chemical Probe of the Inclusion Geometry in the Solid State. Compared to the above-mentioned methods, a distinct strategy designed to elucidate the type of inclusion geometries in crystallized complexes containing the two guest enantiomers has been elaborated. It consisted in evaluating the reactivity of each phase at the solid state by means of alcohol oxidation with iodobenzendiacetate (Scheme 2).[40] Reaction conditions were first optimized under microwave activation without host molecules and the stability of the different phases was checked after irradiation (no phase transition or change of composition). This preliminary step showed that the use of 10 equiv of reagent allowed to reduce the irradiation intensity, and therefore the temperature conditions.

In the absence of host molecule, the oxidation reaction occurs with 96% isolated yield. When oxidation experiments were performed in the presence of TMβ-Cd, the crystalline supramolecular complexes were first ground until amorphization (checked by XRPD) in order to optimize the contact surface.[41] Samples with different enantiomeric compositions have been tested, and results are given with Scheme 2. It appears that the reactivity of guest molecules only depends on the initial crystal packing and is not related to the initial enantiomeric composition: oxidation is observed with a good yield only for the initial phase β, whatever the proportion of guest enantiomers. A blank experiment performed with a physical mixture of the two solid forms confirmed these results, leading to an intermediate

SCHEME 2: Oxidation of the Secondary Alcohol Group of *p*BrPE in the Solid State as a Function of the Initial Crystalline Phase of TMβ-Cd Inclusion Complexes, for Different Enantiomeric Compositions of *p*BrPE

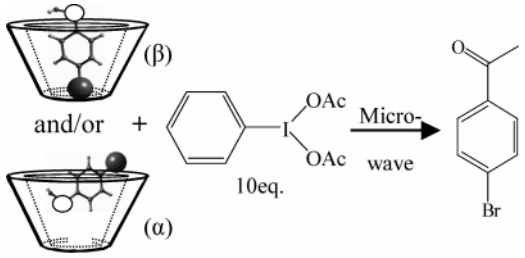

Complex composition (e.e.)	Phase type	Yield
100% (*S*)	α	<5%
100% (*R*)	β	94%
45/55 (*R*/*S*)	α	<5%
54/46 (*R*/*S*)	β	90%
Physical mixture of α and β (1:1)		46%

reactivity. It can be deduced that each crystal form contains only one specific inclusion geometry, allowing or not the oxidation reaction to occur. The alcohol function in phase α is more engulfed in the cyclodextrin cavity and is therefore less accessible, whereas in phase β, the alcohol group is readily

TABLE 2: Solubility Values of Enantiomerically Pure Complexes Formed between TMβ-Cd and *p*BrPE in Water at 40 °C as a Function of the Crystal Form (Controlled by Seeding; Accuracy (±0.15%))

	TMβ-Cd/(*S*)-*p*BrPE		TMβ-Cd/(*R*)-*p*BrPE	
crystal form	$P2_12_12_1$	$P2_1$	$P2_12_12_1$	$P2_1$
	phase α	phase β	phase α	phase β
solubility (w/w in %)	1.2	1.4	2.5	2.4

available for the chemical transformation. Hence, the oxidation reaction acts as a chemical probe to distinguish the inclusion geometries at a molecular scale, since the ability of the host to act as a protecting group depends on the inclusion geometry, initially related to the crystal packing. These data support the initial hypothesis consisting of the existence of 'solid solution' behaviors built with an unique inclusion geometry for a given crystalline phase, whatever the guest enantiomeric composition.

III.2.3. Control of the Inclusion Geometry by the Crystal Packing. Further investigations in this system consisted of attempts to control the inclusion geometry by seeding moderately supersaturated solutions. Powders were analyzed by XRPD and compared with reference data, revealing that the crystal packing can be efficiently controlled irrespective of the initial enantiomeric composition. Stable and metastable solubilities of the two diastereomeric complexes have been evaluated at 40 °C by gravimetric method (Table 2), and are consistent with the existence of two complete solid solutions in the corresponding ternary system.

The solubility values should allow to rationalize the crystallization behavior of TMβ-Cd/*p*BrPE complexes occurring by homogeneous primary nucleation.[42] For phase α, obtained by spontaneous nucleation in close-to-equilibrium conditions, the inclusion geometry in crystalline complexes differs from that existing in solution, which induces a necessary change of the inclusion geometry during nucleation and growth of this low solubility form. By contrast, when spontaneous crystallization occurs under kinetic control because of a higher initial supersaturation, the required inclusion geometry should be a more difficult state to reach. In order to confirm this hypothesis, crystallization experiments of supramolecular complexes formed with the (*S*)-*p*BrPE guest enantiomer have been performed at 40 °C with different initial relative supersaturations (2.2, 2.5, 2.7, 3). XRPD analyses revealed that phase α is obtained for supersaturations lower than 2.7, whereas spontaneous (i.e., unseeded) crystallization leads to phase β for higher values.

When various proportions of the two guest enantiomers are present, it is likely that the supersaturation required to observe the switch from one phase to the other is highly sensitive to the enantiomeric guest proportions. For a racemic composition, phase β is obtained spontaneously for any supersaturation value superior to 2, probably in connection with the ability of both enantiomers to participate to the nucleation mechanism of this phase.

III.2.4. Discrimination Mechanisms and Ternary Phase Diagram. In order to obtain information about the ability of α and β packings to resolve racemic mixtures, further solubility measurements have been performed after successive recrystallization experiments. These data were used to depict the isothermal section of the ternary phase diagram at 40 °C formed between water and the two diastereomeric components (Figure 8). In order to minimize the effect of supersaturation on the resulting crystal packing, only slightly supersaturated solutions were used. The limits between two-phase and three-phase domains have been deduced from the orientation of the tie-lines.

The ternary solubility diagram of this system clearly supports the previous hypothesis about the existence of two complete solid solutions. Since the enantiomeric enrichment during crystallization of each phase is directly related to the tie-line orientations,[43] these data also confirm the higher enantiodiscrimination of phase α.

IV. Extended Discussion on Crystallization Mechanisms and Chiral Discrimination

The data collected in the different sections of this paper, in combination with previous results and interpretations,[16] provide new insights for the understanding of the enantiomeric resolution of (±)-*p*BrPE induced by crystallization of host−guest complexes formed with TMβ-Cd. In particular, it appears that three distinct aspects have to be considered:

1. The efficiency of chiral discrimination is mainly determined by the selectivity of each diastereomeric phase. The orientation of the tie-lines in Figure 8 is consistent with previously published crystal growth results, confirming that phase α is significantly more selective than phase β. Descriptions of crystal structures and molecular modeling investigations have shown that inclusion geometries contribute to the discrimination ability of each phase,[16] whereas crystal packings may also provide a certain enantiomeric recognition through a number of weak intermolecular interactions between neighboring complexes.

2. Chiral resolution is therefore strongly affected by crystallization mechanisms of solid phases. From the results presented above, the primary nucleation step can be rationalized by considering the solvated state and the influence of supersaturation. These aspects are presented in Scheme 3, showing that the proportion of dissociated complexes in solution is quite high, and illustrating that the predominant inclusion geometry of solvated complexes is the same as that depicted in phase β. In the absence of seeding, phase β is therefore favored at high relative supersaturation because it is constituted of host−guest associations similar to that existing in solution, inducing that no reorientation of the guest molecule is necessary prior to the incorporation of the complex in the crystal lattice.[44] By contrast, phase α can only be obtained at low relative supersaturations, since its spontaneous nucleation requires the aggregation in solution of a sufficient amount of host−guest associations with a suitable geometry.

3. From the solubility curves depicted in Figure 8, the role of stable and metastable equilibria can be envisaged as a function of the diastereomeric excess. In particular, the higher ability of phase α for chiral discrimination may be related to the larger solubility difference between the two phases for the higher proportions of (*S*)-*p*BrPE, whereas a low solubility difference is observed for low contents of (*S*)-*p*BrPE. For the racemic composition, the Ostwald's rule of stages seems to be in contradiction with the experimental observations. It is stated in this rule that a system left out of equilibrium evolves toward the closest equilibrium, not toward the most stable one. At racemic composition, phase β is the less soluble and therefore the most stable phase, but it is reproducibly obtained at very high relative supersaturations ($\beta = C/Cs \gg 2$). However, this

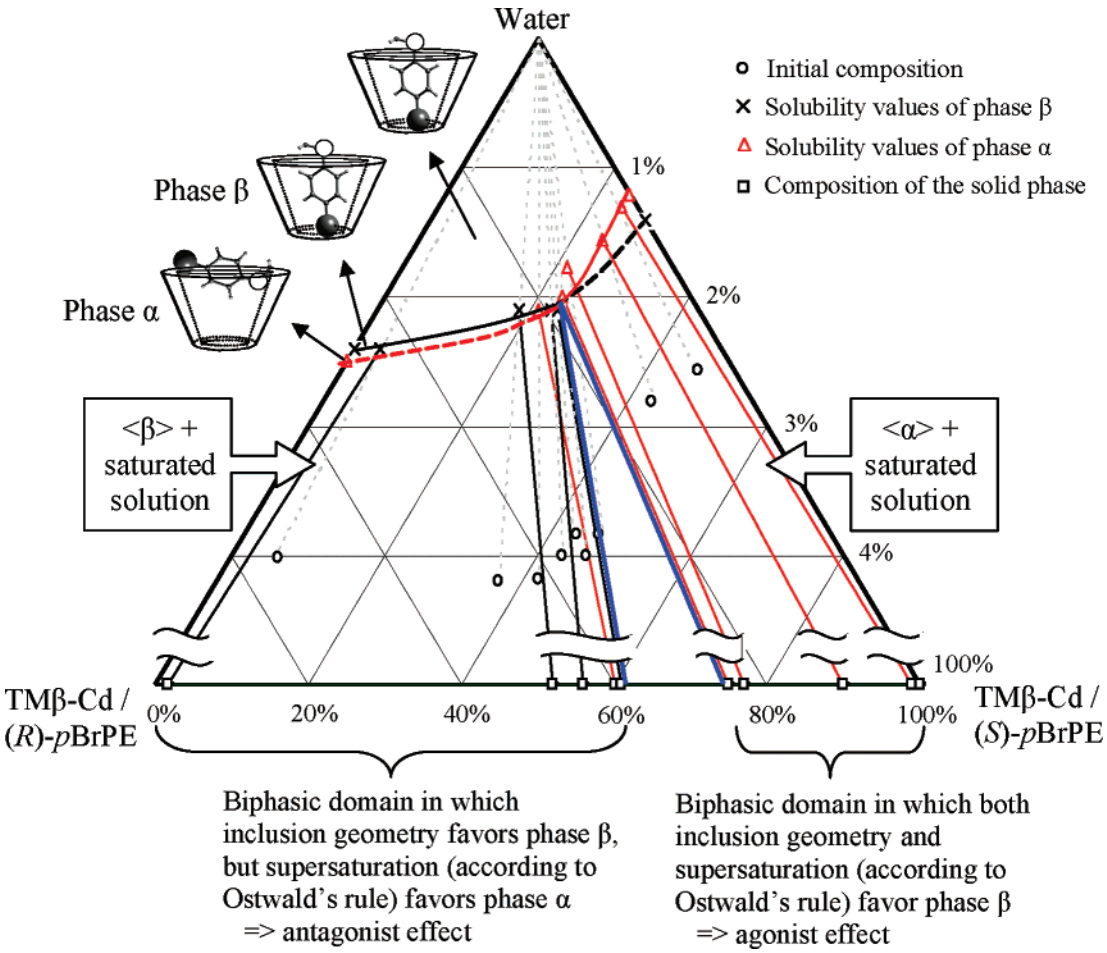

Figure 8. Partial ternary phase diagram formed between water and the two enantiomerically pure complexes (TM*β*-Cd/*p*BrPE) showing the solubility isotherms at 40 °C, and hypothetical domain limits (in blue) deduced from the distribution of tie-lines.

SCHEME 3: Different Steps Involved in Nucleation Mechanisms of Complexes Formed between TM*β*-Cd and *p*BrPE[a]

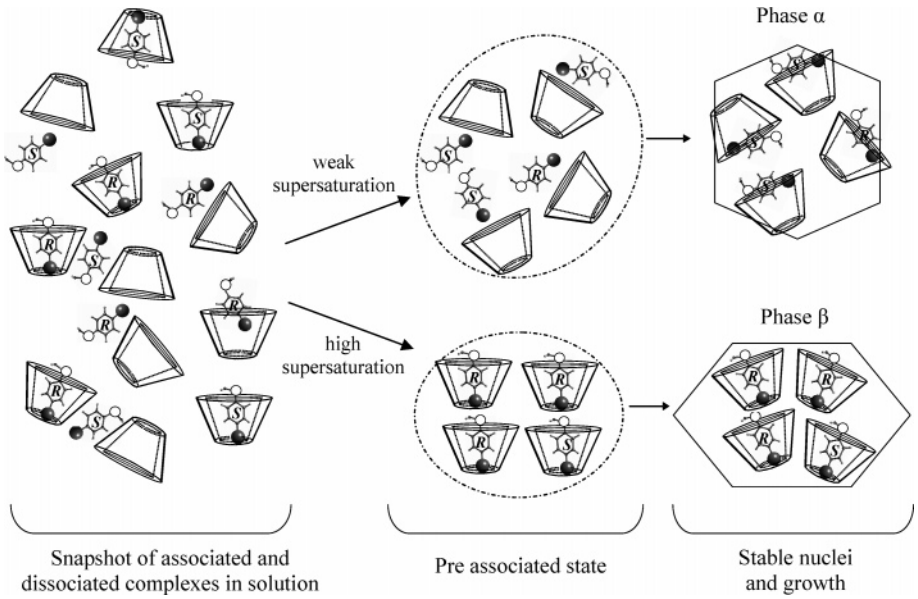

[a] Water molecules are omitted for clarity, and guest distributions in the pre-associated and embryo state were arbitrary chosen.

apparent contradiction can be rationalized for the experimental data provided in the present paper, through the relationship established between the overwhelming inclusion geometry in solution and the host−guest geometry depicted in the two crystal structures.

Hence, the influence of kinetic factors on nucleation and crystal growth probably includes several types of phenomena, and the balance between two of them is shown in Figure 8: in the biphasic domain containing an excess of (*R*)-*p*BrPE, the predominant molecular geometry and the Ostwald's rule cor-

respond to antagonist effects. It should also be mentioned that the diastereomeric excess and the molecular self-assemblies formed in solution could play a decisive role for the nucleation behavior of the two crystalline phases, and could be involved in the chiral recognition occurring at crystal-solution interfaces during the growth of each phase.

V. Conclusion

The characterization of host−guest supramolecular complexes formed in solution between TMβ-Cd and *p*BrPE enantiomers revealed that the crystallization behavior and the structural features of the corresponding complexes cannot be readily inferred from the solvated state. Indeed, a single inclusion geometry was found for the two diastereomeric complexes, with weak binding constants probably associated to a dynamic equilibrium involving simultaneous dissociations and reassociations. The absence of significant chiral discrimination in the solvated state is consistent with the existence of two solid solutions whose solubilities depend on the e.e. of the guest molecule, as shown from the isotherm at 40 °C in the ternary phase diagram. Solid-state NMR and oxidation (used here as a chemical probe to reach structural information) confirmed that a homogeneous distribution of inclusion geometries exists in the two solid solutions.

As a consequence of these new data, the apparent contradiction between the Ostwald's rule of stages and the crystallization behavior of TMβ-Cd/*p*BrPE complexes at racemic composition can be rationalized by comparing the inclusion geometries in solution and in crystal structures. Furthermore, the possibility to resolve racemic *p*BrPE by crystallization of host−guest complexes can only be understood by considering the nucleation of each crystalline phase as the key step for chiral discrimination, and by assuming that the selectivity of each crystal packing is sufficient to account for the enantiomeric enrichments previously observed during successive crystallizations. This detailed case study also highlights that enantiodiscrimination in the solvated state is not a prerequisite for chiral resolution by crystallization of host−guest complexes since the structural and enantiomeric features of a crystalline phase are predominantly determined by the nucleation conditions. It should also be mentioned that crystallization-induced chiral discrimination could be enhanced by kinetic factors, for instance through a large difference between the width of metastable zones of supersaturated systems, inducing that the spontaneous nucleation of one diastereomeric complex only is significantly delayed. This possibility has been recently noticed by Bakirci and Nau,[7] but not fully exploited yet.

Acknowledgment. We thank Prof. Schinzer for the use of NMR facilities at the Institute of Chemistry, Otto-von-Guericke University of Magdeburg (D), and Région Haute-Normandie (F) for financial support to the PhD thesis of Arnaud Grandeury. Dr C. T. Craescu, from the Curie Institute (University of Paris VI, France), is acknowledged for its contribution to Circular Dichroism and Isothermal Titration Calorimetry (ITC) measurements.

Supporting Information Available: Circular dichroism spectrum of TMβ-CD/*p*-Br-PE complexes, and formulas for the calculation of binding constants. This material is available free of charge via the Internet at http://pubs.acs.org.

References and Notes

(1) (a) Lehn, J. M. *Supramolecular Chemistry*; Wiley-VCH: Weinheim, Germany, 1995; pp 11−30. (b) Fisher, E. *Ber. Chem. Ges.* **1905**, *38*, 605. (c) Fisher, E. *Ber. Dtsch. Chem. Ges. 2* **1907**, *40*, 1754.

(2) Harata, K. *Trends Phys. Chem.* **1990**, *1*, 45−57.

(3) (a) Saenger, W. *Angew. Chem., Int. Ed. Engl.* **1980**, *19*, 344−362. (b) Szejtli, J. *Chem. Rev.* **1998**, *98*, 1743−1753. (c) Saenger, W.; Jacob, J.; Gessler, K.; Steiner, T.; Hoffmann, D.; Sanbe, H.; Koizumi, K.; Smith, S. M.; Takaha, T. *Chem. Rev.* **1998**, *98*, 1787−1802.

(4) Liu, L.; Guo, Q.-X. *J. Inclusion Phenom. Macrocyclic Chem*. **2002**, *42*, 1−14.

(5) (a) Wenz, G. *Angew. Chem., Int. Ed. Engl.* **1994**, *33*, 803−822. (b) Rauf Khan, A.; Forgo, P.; Stine, K. J.; D'Souza, V. T. *Chem. Rev.* **1998**, *98*, 1977−1996.

(6) (a) Cramer, F.; Dietsche, W. *Chem. Ber.* **1959**, *92*, 378−385. (b) Benshop, H. P.; Van den Berg, G. R. *J. Chem. Soc., Chem. Commun*. **1970**, 1431−1432. (c) Mikolajczyk, M.; Drabowicz, J. *J. Am. Chem. Soc.* **1978**, *100*, 2510−2515. (d) Hamilton, J. A.; Chen, L. *J. Am. Chem. Soc.* **1988**, *110*, 4379−4391. (e) Hamilton, J. A.; Chen, L. *J. Am. Chem. Soc.* **1988**, *110*, 5833−5841. (f) Rysanek, N.; Le Bas, G.; Villain, F.; Tsoucaris, G. *Acta Cryst.* **1992**, *C48*, 1466−1471. (g) Alexander, J. M.; Clark, J. L.; Brett, T. J.; Stezowski, J. J. *Proc. Natl. Acad. Sci. U.S.A.* **2002**, *99*, 5115−5120.

(7) Bakirci, H.; Nau, W. M. *J. Org. Chem.* **2005**, *70*, 4506−4509.

(8) Arad-Yellin, R.; Green, B. S.; Knossow, M.; Tsoucaris, G. *Inclusion Compounds III*; Academic Press: London, 1984; pp 278−284.

(9) Harata, K. *Chem. Rev.* **1998**, *98*, 1803−1827.

(10) Jacques, J.; Collet, A.; Willen, S. H. *Enantiomers, Racemates and Resolutions*, 2nd ed.; Kriger Publishing Company: Malabar, FL, 1994.

(11) (a) Lipkowitz, K. B.; Gree, K. M.; Yang, J.-A.; Peterson, M. A. *Chirality* **1993**, *5*, 51−57. (b) Reinhart, R.; Richter, M.; Mager, P. P. *Carbohydr. Res.* **1996**, *291*, 1−9.

(12) (a) Kano, K.; Yoshiyasu, K.; Hashimoto, S. *J. Chem. Soc., Chem. Commun.* **1989**, 1278−1279. (b) Kano, K.; Kato, Y.; Kodera, M. *J. Chem. Soc., Perkin Trans. 2* **1996**, 1211−1216.

(13) (a) Yannakopoulou, K.; Mentzafos, D.; Dandika, K.; Mavridis, I. M. *Angew. Chem., Int. Ed. Engl.* **1996**, *35*, 2480−2483. (b) Makedonopoulou, S.; Yannakopoulou, K.; Mentzafos, D.; Lamzin, V.; Popov, A.; Mavridis, I. M. *Acta Crystallogr.* **2001**, *B57*, 399−409.

(14) Ferron, L.; Guillen, F.; Coste, S.; Coquerel, G.; Plaquevent, J.-C. *Chirality* **2006**, *18*, 662−666.

(15) Grandeury, A.; Tisse, S.; Gouhier, G.; Agasse, V.; Petit, S.; Coquerel, G. *Chem. Eng. Technol.* **2003**, *26*, 354−358.

(16) Grandeury, A.; Petit, S.; Gouhier, G.; Agasse, V.; Coquerel, G. *Tetrahedron: Asymmetry* **2003**, *14*, 2143−2152.

(17) Grandeury, A.; Renou, L.; Dufour, F.; Petit, S.; Gouhier, G.; Coquerel, G. *J. Therm. Anal. Calorim.* **2004**, *77*, 377−390.

(18) Polavarapu, P. L.; Fontana, L. P.; Smith, H. E. *J. Am. Chem. Soc.* **1986**, *108*, 94−99.

(19) (a) Aue, W. P.; Bartholdi, E.; Ernst, R. R. *J. Chem. Phys.* **1976**, *64*, 2229−2246. (b) Hurd, R. E. *J. Magn. Reson.* **1990**, *87*, 422−428.

(20) (a) Bax, A.; Griffey, R. H.; Hawkins, B. L. *J. Magn. Reson.* **1983**, *55*, 301−315. (b) Bax, A.; Subramanian, S. *J. Magn. Reson.* **1986**, *67*, 565−569.

(21) (a) Bax, A.; Summers, M. F. *J. Am. Chem. Soc.* **1986**, *108*, 2093−2094. (b) Willker, W.; Leibfritz, D.; Kerssebaum, R.; Bermel, W. *Magn. Reson. Chem.* **1993**, *31*, 287−292.

(22) (a) Jeener, J.; Meier, B. H.; Bachmann, P.; Ernst, R. R. *J. Chem. Phys.* **1979**, *71*, 4546−4553. (b) Parella, T.; Sanchez-Ferrando, F.; Virgili, A. *J. Magn. Reson.* **1997**, *125*, 145−148.

(23) (a) Bax, A.; Davis, D. G. *J. Magn. Reson.* **1985**, *63*, 207−213. (b) Hwang, T. L.; Shaka, A. J. *J. Am. Chem. Soc.* **1992**, *114*, 3157−3159.

(24) Kowalewski, J.; Levy, G. C.; Johnson, L. F.; Palmer, L. *J. Magn. Reson.* **1977**, *26*, 533−536.

(25) Schneider, H.-J.; Hacket, F.; Rudiger, V.; Ikeda, H. *Chem. Rev.* **1998**, *98*, 1755−1785.

(26) (a) Uekama, K.; Irie, T. In *Cyclodextrins and their Industrial Uses*; Duchene, D., Ed.; Editions de Santé: Paris, 1987; pp 393−439. (b) Starikov, E. B.; Brasicke, K.; Knapp, E. W.; Saenger, W. *Chem. Phys. Lett.* **2001**, *336*, 504−510.

(27) (a) Alderfer, J. L.; Eliseev, A. V. *J. Org. Chem.* **1997**, *62*, 8225−8226. (b) Shibakami, M.; Sekiya, A. *J. Chem. Soc., Chem. Commun*. **1992**, 1742−1743.

(28) Liu, L.; Li, X.-S.; Guo, Q.-X. *J. Mol. Struct. (THEOCHEM*) **2000**, *530*, 31−37.

(29) (a) Connors, K. *Binding Constant*; Wiley and Sons: New York, 1987. (b) Horman, I.; Dreux, B. *Helv. Chim. Acta.* **1984**, *67*, 754−764.

(30) (a) Rekharsky, M.; Inoue, Y. *J. Am. Chem. Soc.* **2000**, *122*, 4418−4435. (b) Rekharsky, M.; Inoue, Y. *J. Am. Chem. Soc.* **2000**, *122*, 10949−10955. (c) Rekharsky, M.; Inoue, Y. *J. Am. Chem. Soc.* **2002**, *124*, 813−826.

(31) (a) Höfler, T.; Wenz, G. *J. Incl. Phen. Mol. Recogn. Chem.* **1996**, *25*, 81−84. (b) Piel, G.; Moutard, S.; Perly, B.; de Hassonville, S. H.;

Bertholet, P.; Barillaro, V.; Piette, M.; Delattre, L.; Evrard, B. *J. Drug Deliv. Sci. Technol.* **2004**, *14*, 87−91.

(32) (a) Kammerer, H.; Horner, L.; Beck, L. *Chem. Ber.* **1958**, *91*, 1376−1379. (b) Tahiro, M.; Nakamura, H.; Nakayama, K. *Org. Prep. Proced. Int.* **1987**, *19*, 442−446.

(33) Fini, P.; Castagnolo, M.; Catucci, L.; Cosma, P.; Agostiano, A. *J. Therm. Anal. Cal.* **2003**, *73*, 653−659.

(34) (a) Ripmeester, J. A.; Burlinson, N. E. *J. Am. Chem. Soc.* **1985**, *107*, 3713−3714. (b) Ripmeester, J. A.; Ratcliffe, C. I.; Cameron, I. G. *Carbohydr. Res.* **1989**, *192*, 69−81.

(35) Wood, D. J.; Hruska, F. E.; Saenger, W. *J. Am. Chem. Soc.* **1977**, *99*, 1735−1740.

(36) (a) Gidley, M. J.; Bociek, S. M. *J. Am. Chem. Soc.* **1988**, *110*, 3820. (b) Ripmeester, J. A.; Ratcliffe, C. I. In *Comprehensive Supramolecular Chemistry*; Davies, J. E. D., Ripmeester, J. A., Eds.; Elsevier: Oxford, 1996; Vol. 8, pp 323−380.

(37) Caira, M. R.; Griffith, V. J.; Nassimbeni, L. R.; Outshoom, B. V. *J. Chem. Soc., Perkin Trans. 2* **1994**, 2071−2072.

(38) Petrovski, Z.; Braga, S. S.; Santos, A. M.; Rodrigues, S. S.; Goncalves, I. S.; Pillinger, M.; Kuhn, F. E.; Romao, C. C. *Inorg. Chim. Acta* **2005**, 981−988.

(39) Braga, S. S.; Marques, M. P.; Sousa, J. B.; Pillinger, M.; Teixeira-Dias, J. J. C.; Goncalves, I. S. *J. Organometal. Chem.* **2005**, *690*, 2905−2912.

(40) Varma, R. S.; Dahiya, R.; Saini, R. K. *Tetrahedron Lett.* **1997**, *38*, 7029−7032.

(41) Grandeury, A.; Petit, S.; Coste, S.; Coquerel, G.; Perrio, C.; Gouhier, G. *Chem. Comm.* **2005**, *31*, 4007−4009.

(42) Threlfall, T. *Org. Proc. Res. Dev.* **2003**, *7*, 1017−1027.

(43) Marchand, P.; Lefebvre, L.; Querniard, F.; Cardinael, P.; Perez, G.; Counioux, J.-J.; Coquerel, G. *Tetrahedron: Asymmetry* **2004**, *15*, 2455−2465.

(44) (a) Petit, S.; Coquerel, G.; Hartman, P. *J. Cryst. Growth* **1994**, *137*, 585−594. (b) Davey, R. J.; Blagden, N.; Righini, S.; Alison, H.; Quayle, M. J.; Fuller, S. *Cryst. Growth Des.* **2001**, *1*, 59−65.